White Matter Hyperintensities Are a Core Feature of Alzheimer's Disease: Evidence from the Dominantly Inherited Alzheimer Network

Seonjoo Lee, PhD,[1,2] Fawad Viqar, MA,[3,4] Molly E. Zimmerman, PhD,[4,5]
Atul Narkhede, MS,[3] Giuseppe Tosto, MD, PhD,[3,6]
Tammie L.S. Benzinger, MD, PhD,[7] Daniel S. Marcus, PhD,[7]
Anne M. Fagan, PhD,[8] Alison Goate, PhD,[9] Nick C. Fox, MD,[10]
Nigel J. Cairns, PhD,[11] David M. Holtzman, MD,[8] Virginia Buckles, PhD,[8]
Bernardino Ghetti, MD,[12] Eric McDade, DO,[8] Ralph N. Martins, PhD,[13]
Andrew J. Saykin, PsyD,[14] Colin L. Masters, MD,[15] John M. Ringman, MD,[16]
Natalie S. Ryan, MBBS,[10] Stefan Förster, MD,[17] Christoph Laske, MD,[18]
Peter R. Schofield, PhD, DSc,[19] Reisa A. Sperling, MD,[20] Stephen Salloway, MD,[21]
Stephen Correia, PhD,[22] Clifford Jack Jr. MD,[23] Michael Weiner, MD,[24]
Randall J. Bateman, MD,[8] John C. Morris, MD,[8] Richard Mayeux, MD,[3,6,25]
and Adam M. Brickman, PhD,[3,6,25] for the Dominantly Inherited Alzheimer Network

From the [1]Department of Psychiatry, College of Physicians and Surgeons, Columbia University, New York, NY; [2]Division of Biostatistics, New York State Psychiatric Institute, New York, NY; [3]Taub Institute for Research on Alzheimer's Disease and the Aging Brain, College of Physicians and Surgeons, Columbia University, New York, NY; [4]Psychology Department, Fordham University, Bronx, NY; [5]Department of Neurology, Albert Einstein College of Medicine, Bronx, NY; [6]Department of Neurology, Columbia University Medical Center and the New York Presbyterian Hospital, Columbia University, New York, NY; [7]Department of Radiology, Washington University School of Medicine, Saint Louis, MO; [8]Department of Neurology, Washington University School of Medicine, St. Louis, MO; [9]Department of Neuroscience, Icahn School of Medicine at Mount Sinai, New York, NY; [10]Dementia Research Center, Department of Neurodegenerative Disease, UCL Institute of Neurology, London, United Kingdom; [11]Department of Pathology and Immunology, Washington University School of Medicine, St. Louis, MO; [12]Department of Pathology and Laboratory Medicine, Indiana University School of Medicine, Indianapolis, IN; [13]Center of Excellence of Alzheimer's Disease Research and Care, School of Exercise, Biomedical and Health Sciences, Edith Cowan University, Perth, Australia; [14]Indiana Alzheimer Disease Center and Department of Radiology and Imaging Sciences, Indiana University School of Medicine, Indianapolis, IN; [15]The Florey Institute, University of Melbourne, Parkville, Australia; [16]Memory and Aging Center, Keck School of Medicine of University of Southern California, Los Angeles, CA; [17]German Center for Neurodegenerative Diseases (DZNE) München and Tübingen and Department of Nuclear Medicine, Technische Universität München (TUM), Munich, Germany; [18]German Center for Neurodegenerative Diseases (DZNE) and the Section for Dementia Research, Department of Cellular Neurology, Hertie Institute for Clinical Brain Research and Department of Psychiatry and Psychotherapy, University of Tübingen, Tübingen, Germany; [19]Neuroscience Research Australia and University of New South Wales, Sydney, Australia; [20]Center for Alzheimer Research and Treatment, Brigham and Women's Hospital and Massachusetts General Hospital, Boston, MA; [21]Butler Hospital and Department of Neurology, Alpert Medical School, Brown University, Providence, RI; [22]Department of Psychiatry, Alpert Medical School, Brown University, Providence, RI; [23]Department of Radiology, Mayo Clinic, Rochester, MN; [24]Department of Radiology and Biomedical Imaging, Center for Imaging of Neurodegenerative Diseases, San Francisco Veterans Affairs Medical Center and Departments of Psychiatry, Radiology, Medicine, and Neurology, University of California at San Francisco, San Francisco, CA; and [25]Gertrude H. Sergievsky Center, College of Physicians and Surgeons, Columbia University, New York, NY

Additional supporting information can be found in the online version of this article.

Objective: White matter hyperintensities (WMHs) are areas of increased signal on T2-weighted magnetic resonance imaging (MRI) scans that most commonly reflect small vessel cerebrovascular disease. Increased WMH volume is associated with risk and progression of Alzheimer's disease (AD). These observations are typically interpreted as evidence that vascular abnormalities play an additive, independent role contributing to symptom presentation, but not core features of AD. We examined the severity and distribution of WMH in presymptomatic *PSEN1*, *PSEN2*, and *APP* mutation carriers to determine the extent to which WMH manifest in individuals genetically determined to develop AD.

Methods: The study comprised participants (n = 299; age = 39.03 ± 10.13) from the Dominantly Inherited Alzheimer Network, including 184 (61.5%) with a mutation that results in AD and 115 (38.5%) first-degree relatives who were noncarrier controls. We calculated the estimated years from expected symptom onset (EYO) by subtracting the affected parent's symptom onset age from the participant's age. Baseline MRI data were analyzed for total and regional WMH. Mixed-effects piece-wise linear regression was used to examine WMH differences between carriers and noncarriers with respect to EYO.

Results: Mutation carriers had greater total WMH volumes, which appeared to increase approximately 6 years before expected symptom onset. Effects were most prominent for the parietal and occipital lobe, which showed divergent effects as early as 22 years before estimated onset.

Interpretation: Autosomal-dominant AD is associated with increased WMH well before expected symptom onset. The findings suggest the possibility that WMHs are a core feature of AD, a potential therapeutic target, and a factor that should be integrated into pathogenic models of the disease.

White matter hyperintensities (WMHs), visualized as increased signal on T2-weighted magnetic resonance imaging (MRI) of the brain are common radiological features of aging. Previously thought to reflect benign changes in underlying tissue or radiographic artifacts, they have emerged as correlates of cognitive, functional, emotional, and motoric abnormalities that emerge in later life[1] and have been linked pathologically to small vessel cerebrovascular disease, including arteriosclerosis, demyelination, and axonal loss attributed to ischemia or neuronal death, cerebral amyloid angiopathy, and microglia activation.[2] In recent years, there has been strong evidence that WMHs are associated with the clinical risk and symptomatic course of late-onset Alzheimer's disease (LOAD).[3] Despite these consistent observations, white matter abnormalities are not included in current conceptual models of the pathogenesis and biological marker progression of LOAD (e.g., a previous work[4]). The debate on the extent to which WMHs represent a core feature of LOAD can be summarized in two opposing views. On the one hand, because Alzheimer's disease (AD) is defined pathologically by the presence of amyloid-beta (Aβ) plaques with neuritic plaques and neurofibrillary tangles adding to the severity of the changes, white matter damage is considered a comorbidity that does not represent these pathologies. On the other hand, WMHs predict the clinical onset and course of AD similarly to, or better than, other biological markers of AD,[5,6] may, in part, reflect vascular forms of AD pathology, there are viable biological models that implicate small vessel cerebrovascular disease in the deposition of primary AD pathology,[7] and among individuals with late-onset dementia, presence of multiple pathologies is more common than not.[8–10]

The study of the emergence of WMH—or any biological markers—and their contributions to LOAD in humans is difficult because the ordering and timing of the biological changes that lead to dementia can occur up to decades before the onset of symptoms,[4] which is typically the point when human studies of LOAD are conducted. WMH severity is also tightly linked to vascular risk factors and age,[2] so determination of its contribution to LOAD is potentially confounded by these factors. To overcome these issues, we turned to the landmark Dominantly Inherited Alzheimer Network (DIAN) study. The study enrolls individuals at 50% risk for autosomal-dominant AD by virtue of having a first-degree relative with a pathogenic mutation in one of three AD-causing genes: amyloid precursor protein (*APP*); presenilin 1 (*PSEN1*); and presenilin 2 (*PSEN2*). Pathogenic mutations are virtually fully penetrant, leading to 100% probability that the mutation carrier will develop early-onset AD. Although autosomal-dominant forms of AD account for fewer than 1% of all AD cases, there is strong overlap in symptomatology with LOAD, and a recent critical DIAN study established that the order of biological changes begins with deposition of amyloid, followed by neurodegenerative changes (e.g., as indexed by levels of tau protein in the cerebrospinal fluid [CSF]), and cognitive decline.[11] Because age at onset of clinical symptoms is highly heritable among individuals with autosomal-dominant AD,[12] parental age at onset can be used as a reliable estimate of clinical onset among asymptomatic mutation carriers. Here, we tested the hypothesis that WMH burden is elevated among mutation carriers and increases with greater temporal proximity to the estimated year of onset of clinical symptoms. Our goal was to determine definitively whether WMHs are a core feature of AD. Given our previous observations of a WMH

regional selectivity in LOAD, we also examined the regional distribution of WMH.

Patients and Methods

Overall Design

The DIAN study (www.dian-info.org; NIA-U19-AG032438) is an international effort that includes sites in the United States, UK, Germany, and Australia. The study recruits individuals from families with a known autosomal-dominant mutation for AD, including *APP, PSEN1,* and *PSEN2,* irrespective of their own mutation status. As part of the DIAN Observational Study, participants receive a baseline assessment with sampling of blood and CSF, clinical assessment, neuropsychological evaluation, and neuroimaging and are followed longitudinally with identical assessments. Full procedures for the study are described elsewhere.[11,13] All study procedures received approval from each participating institution, and all participants gave informed consent.

Clinical Assessment

All evaluation procedures were conducted by individuals unaware of the mutation status of each participant. Clinical assessment included evaluation with the Clinical Dementia Rating scale (CDR),[14] physical and neurological examination, neuropsychological testing, and determination of parental age at onset. Parental age at onset was determined with a semistructured interview that assessed the age at which the affected parent began exhibiting signs of progressive cognitive decline.[11] Estimated years from expected symptom onset (EYO) were calculated as the difference between the participant's age and parental age at onset.[11] This variable was established for all participants regardless of their own mutation status. Data included in the present study were a subset from Data Freeze 6 with available T2-weighted MRI scans. Remote or current history of hypertension, hypercholesterolemia, diabetes, and smoking (≥100 cigarettes smoked in lifetime) was ascertained by interview and considered in secondary analyses.

Biochemical and Genetic Analysis

CSF was collected via lumbar puncture on each participant under fasting conditions.[11] Samples were shipped to the DIAN biomarker core laboratory, and immunoassay (INNOTEST β-Amyloid$_{1-42}$ and INNO-BIA AlzBio3) was used to measure CSF concentrations of Aβ_{1-42} and phosphorylated tau (ptau181). All samples underwent quality-control procedures.[11] Each participant's mutation status and *APOE* genotype was determined according to procedures in the published DIAN protocol.[11,13]

Brain Imaging

Participants received structural MRI. For the current study, we quantified WMH on T2-weighted fluid-attenuated inversion recovery (FLAIR) structural MRI scans. Scan acquisition took place on prequalified 3 Tesla scanners at each site. Harmonization and quality assurance across platforms, sites, and acquisition times followed the Alzheimer's Disease Neuroimaging Initiative (ADNI) protocols.[15] The neuroimaging core laboratory reviewed each MRI scan to ensure compliance with the acquisition protocol and image quality. Standardized FLAIR sequences (repetition time, 9,000; echo time, 90; inversion time, 2,500; voxel dimensions: 0.86 × 0.86 × 5.0 mm) were acquired as part of the DIAN MRI protocol. FLAIR images were transferred to Columbia University (New York, NY) for WMH quantification using procedures previously described.[16] Briefly, a study-specific intensity threshold was applied to each image to label voxels falling within the WMH intensity distribution. An expert operator reviewed and edited every image, if necessary. A "lobar" atlas was coregistered linearly to each labeled FLAIR image to define WMH volumes in frontal, temporal, parietal, and occipital lobes. WMH volume was defined as the sum of the labeled voxels multiplied by voxel dimensions; regional volumes were calculated within each labeled lobar region of interest. In a random subset of 10 participants, test-retest reliability was greater than 0.98 for regional and total WMH volumes. All imaging analyses were completed without knowledge of mutation status and demographic and clinical data.

In a subset of participants, T2*-weighted MR images were analyzed at the Mayo Clinic (Rochester, MN) for presence of cerebral microbleeds. We operationally defined possible cerebral amyloid angiopathy (CAA) as the presence of at least one cerebral microbleed according to the Boston criteria.[17] We examined whether the presence of cerebral microbleeds mediated the hypothesized relationship between WMH and mutation status.

Statistical Analysis

Demographic and clinical variables were compared between mutation carriers and noncarriers with *t* tests and chi-squared analysis for continuous and categorical data, respectively. We explored the relationship between total WMH volume and CSF-derived AD biomarkers with Spearman's rank-order correlations stratified by mutation status. To test whether WMH volume differed by mutation type, we used a general linear model that examined the interaction between carrier status (carrier vs. noncarrier) and familial mutation type (*PSEN1, PSEN2,* and *APP*). We employed piece-wise linear mixed-effect regression with an inflection point as a parameter[18] to examine the total and regional WMH volumes with respect to estimated years from symptom onset, controlling for participant family as a random effect. The primary parameter of interest was the interaction between mutation status and EYO, which would demonstrate that WMH volume is increasing among mutation carriers at a rate that is greater than non-carriers. The inclusion of the inflection point as an additional parameter, in the context of a significant interaction, tests whether there is a point within the time period at which the association between EYO and WMH volume begins to diverge between mutation carriers and noncarriers. The inflection point was selected based on Bayesian information criterion[19]; we tested whether inclusion of the inflection point significantly improved the model fit compared with the model without the inflection point with the

likelihood ratio test (LRT).[20] Overall model fits were also determined with the LRT. Similar analyses were run with CSF measures of $A\beta_{1-42}$ (a marker of β-amyloid), ptau181 (a presumed marker of neurofibrillary tangles), and the ratio of $A\beta_{1-42}$ to ptau181 in order to compare the timing and ordering among the biomarkers. Analyses involving WMH were also rerun controlling for ptau181 (model 2) or $A\beta_{1-42}$ (model 3). Analyses were rerun after inclusion of participant age and apolipoprotein E (APOE)-ϵ4 status as additional covariates to ensure that the primary observations were not confounded by these factors. Similarly, we compared vascular risk histories between mutation carriers and noncarriers and computed a vascular risk summary score by adding the dichotomous variables together. This score was considered as a covariate in subsequent analyses. For visualization, LOESS regression analysis[21] was conducted and the estimates and their 95% confidence limits were plotted. Statistical analyses were conducted with the use of the PROC MIXED and SGPLOT procedures in SAS software (version 9.3; SAS Institute Inc., Cary, NC). We tested the differences in total and regional WMH volumes in individuals with CDR scores of 0 with a general linear model, adjusting for participant's age, to ensure that differences between groups were not related to the inclusion of symptomatic individuals. Before statistical analyses, total and regional WMH volumes underwent inverse hyperbolic transformation because the distributions of these variables were highly positively skewed.[22]

Similar mixed-effects piece-wise linear regression and formal testing of mediation was used to examine differences between carriers and noncarriers in presence of cerebral microbleeds and to test the whether the association between WMH and mutation status is dependent on the presence of cerebral microbleeds.

Results

Data from 299 participants of the total DIAN cohort that had passed rigorous quality assurance for Data Freeze 6 were included in these analyses (see Table 1 for demographic, clinical, and biomarker data). There were 184 (61.5%) mutation carriers, including 141 (77%) *PSEN1*, 15 (8%) *PSEN2*, and 28 (15%) *APP* mutation carriers. Mutation carriers and noncarriers were almost identical in age, sex distribution, vascular risk factors, EYO, and frequency of APOE-ϵ4, but had a greater proportion of symptomatic individuals (i.e., CDR > 0). Mutation carriers had greater total, temporal, parietal, and occipital WMH volumes than noncarriers; these differences between mutation carriers and noncarriers remained when restricting the sample to asymptomatic participants (i.e., CDR = 0; $p < 0.05$ for total and occipital lobe; $p = 0.09$ for parietal lobe; $p = 0.11$ for temporal lobe). Differences in WMH volume between mutation carriers and noncarriers were not driven by a single mutation type, as evidenced by a significant main effect of carrier status ($p < 0.05$) for WMH in all

regions apart from frontal lobe and nonsignificant interactions ($p > 0.05$) between carrier status and mutation type for all regions. As expected, mutation carriers had lower levels of $A\beta_{1-42}$ and higher levels of ptau181 compared to noncarriers; these differences remained ($p < 0.001$) when restricting the sample to individuals with CDR scores of 0. Increased total WMH volume was associated with lower $A\beta_{1-42}$ levels in mutation carriers (r = −0.190; $p = 0.01$), but not in noncarriers ($r = -0.053$; $p = 0.623$; see Fig 1). WMH volume was not related to ptau181 levels in mutation carriers ($r = -0.090$; $p = 0.162$) or in noncarriers ($r = -0.025$; $p = 0.813$). Descriptive statistics for WMH volume, including median, first quartile, third quartile, and interquartile range (IQR), are presented in Table 2.

Results of the piece-wise linear mixed-effect analyses revealed a reliable increase in total WMH volume among mutation carriers (significant mutation status by EYO interactions) with an inflection point occurring approximately 6.6 years before estimated symptom onset (EYO, −6.6; see Fig 2 and Supplementary Table). When we examined regional distribution of WMH, significant effects emerged in the parietal and occipital lobes. For the parietal lobe, much like total WMH volume, the inflection point occurred approximately 7 years before estimated symptom onset (EYO, −7). For the occipital lobes, the inflection point occurred approximately 22 years before estimated symptom onset (EYO, −22; see Fig 3). CSF levels of $A\beta_{1-42}$, ptau181, and $A\beta_{1-42}$ to ptau181 ratio levels appeared to diverge in mutation carriers approximately 30, 26, and 29 years before estimated symptom onset, respectively. Thus, in terms of ordering and staging, the results suggest that total WMH volumes are increased reliably after amyloid and tau abnormalities are detectable, but before symptom onset. Regionally, posterior WMH volume increases in mutation carriers at around the same time that CSF ptau181 and CSF amyloid changes occur. When adjusting for CSF AD biomarkers, total WMH volumes remained significantly elevated in mutation carriers when controlling for ptau181 levels, but not when controlling for $A\beta_{1-42}$ levels. Figure 4 displays representative examples of WMH in mutation carriers and noncarriers across three EYO time points. When all analyses were repeated with age and APOE-ϵ4 status as additional covariates (data not shown), none of the primary observations were altered and the additional covariate parameters were not statistically significant. Similarly, when analyses were rerun with the vascular risk summary score, none of the primary observations changed.

When we examined the potential contribution of CAA among a subset of participants (n = 175), we found that mutation carriers were more likely to have

TABLE 1. Demographic, Clinical, and Biomarker Data in Mutation Carriers and Noncarriers				
		Mutation Noncarriers	Mutation Carriers	Total Sample	Statistic
N		115	184	299	
Age, mean years ± SD		39.95 ± 9.93	39.09 ± 10.29	39.03 ± 10.13	$t = 0.115$, $p = 0.908$
EYO, mean years ± SD		–7.86 ± 11.57	–7.39 ± 9.51	–7.57 ± 10.34	$t = 0.385$, $p = 0.703$
Women, n (%)		65 (56.5)	104 (56.5)	169 (56.5)	$\chi^2 = 0.00$, $p = 1.00$
Vascular factors (%)	Hypertension	17 (15)	18 (10)	35 (12)	$\chi^2 = 1.3$, $p = 0.26$
	Hypercholesterolemia	20 (17)	28 (15)	48 (16)	$\chi^2 = 0.09$, $p = 0.77$
	Diabetes	2 (1.7)	3 (1.6)	5 (1.7)	$\chi^2 = 0.005$, $p = 0.94$
	Smoking	49 (43)	74 (40)	123 (41)	$\chi^2 = 0.08$, $p = 0.77$
CDR (%)	0	107 (93)	114 (62)	221 (74)	$\chi^2 = 37.31$, $p < 0.001$
	0.5	8 (7)	43 (23)	51 (17)	
	1	0 (0)	20 (11)	20 (6.67)	
	2	0 (0)	5 (3)	5 (1.67)	
	3	0 (0)	2 (1)	2 (0.67)	
APOE-ϵ4+ (%)		33 (29)	56 (30.4)	89 (30)	$\chi^2 = 0.102$, $p = 0.749$
WMH, mean IHS ± SD[a]	Frontal	0.15 ± 0.34	0.47 ± 2.92	0.35 ± 2.30	$t = 1.44$, $p = 0.151$
	Temporal	0.02 ± 0.11	0.12 ± 0.48	0.08 ± 0.39	$t = 2.62$, $p = 0.009$
	Parietal	0.06 ± 0.25	0.41 ± 2.29	0.27 ± 1.811	$t = 2.05$, $p = 0.042$
	Occipital	0.09 ± 0.16	0.33 ± 0.77	0.24 ± 0.62	$t = 4.08$, $p < 0.001$
	Total	0.39 ± 0.73	1.42 ± 6.02	1.03 ± 4.77	$t = 2.29$, $p = 0.023$
CSF Aβ_{1-42}[a,b]		411.40 ± 113.49	304.50 ± 156.85	343.93 ± 151.25	$t = 6.14$, $p < 0.001$
CSF ptau181[a,c]		29.93 ± 10.18	65.58 ± 37.79	52.41 ± 35.12	$t = 11.14$, $p < 0.001$
CSF Aβ_{1-42} :tau ratio		8.123 ±4.23	4.26 ±4.02	5.68 ±4.49	$t = 7.11$, $p < 0.001$

[a]Equal variances not assumed because Levene's test for equality of variances was significant ($p < 0.01$).
[b]Available for n = 244.
[c]Available for n = 249.
APOE = apolipoprotein E; EYO = estimated years to symptom onset; CDR = Clinical Dementia Rating scale; WMH = white matter hyperintensities; IHS = inverse hyperbolic sine; SD = standard deviation.
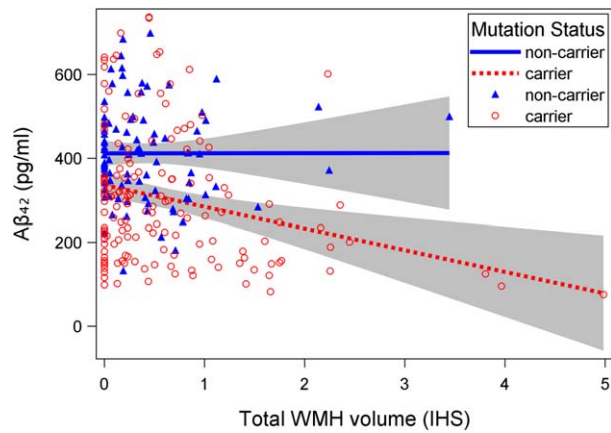
FIGURE 1: Correlation between total WMH volume and $A\beta_{1-42}$, plotted separately for mutation carriers and noncarriers. The relationship was significant ($r = -0.26$; $p = 0.0012$) for carriers, but not for noncarriers ($r = -0.053$; $p = 0.623$). Shaded areas represent 95% confidence intervals. IHS = inverse hyperbolic sine transformation; WMH = white matter hyperintensity. [Color figure can be viewed in the online issue, which is available at www.annalsofneurology.org.]

cerebral microbleeds than noncarriers (20% vs. 6%; $p < 0.05$) and individuals with microbleeds had higher WMH volume than those without ($p < 0.05$). WMH volume was increased in mutation carriers, up to 20 years before EYO, after controlling for microbleed status. Total WMH also remained significantly elevated in mutation carriers even after exclusion of individuals with microbleeds from the study sample. Formal testing of mediation demonstrated that 21% of the association between mutation status and WMH was mediated by presence of microbleeds ($p = 0.03$), but a significant direct effect of WMH remained ($p = 0.02$) after controlling for presence of microbleeds.

Discussion

We found that total WMH volume is significantly elevated among individuals with autosomal-dominant genetic mutations for AD approximately 6 years before their estimated age of symptom onset. When considered regionally, WMH volume distributed in posterior brain areas is selectively elevated among mutation carriers around 22 years before estimated symptom onset. Together with the previous studies that have implicated WMH, particularly in posterior regions, in risk and progression of clinical symptomatology of LOAD,[16,23] our study suggests that WMHs are an important feature of AD. Because mutation carriers and noncarriers in the current study are relatively young, virtually identical demographically, and at identical risk for inheriting an autosomal-dominant mutation by virtue of having a parent with a mutation, the findings provide strong evidence that WMH in this population do not reflect comorbidity or other pathophysiology, but rather reflect primary pathogenic processes in AD. The results highlight the potential role of regionally distributed WMH in AD and point to new avenues of investigation for preventative or treatment strategies.

In the context of other AD biomarkers, WMHs appear to emerge globally after measurable changes in CSF $A\beta_{1-42}$ and ptau181, but before symptom onset, although WMHs distributed in posterior brain areas appear elevated at around the same time as tau and $A\beta_{1-42}$ differences. These findings should be interpreted in the context of wide confidence intervals, and therefore relatively lower reliability related to the inflection point analyses. WMH volume correlated with CSF $A\beta_{1-42}$, but not ptau181, and when controlling for $A\beta_{1-42}$ in our

TABLE 2. Descriptive Statistics of WMH Volume (in cm³), Including Median, First Quartile (Q1), Third Quartile (Q3), and Interquartile Range for Tight Bands of Participants Defined by Estimated Years to Symptom Onset and Stratified by Mutation Status

	Mutation Noncarrier					Mutation Carrier					Total				
EYO	N	Med	Q1	Q3	IQR	N	Med	Q1	Q3	IQR	N	Med	Q1	Q3	IQR
−30 to −20 yr	13	0.19	0.04	0.44	0.40	18	0.41	0.19	0.72	0.54	31	0.24	0.04	0.72	0.68
−20 to −10 yr	40	0.35	0.05	0.79	0.74	52	0.29	0.05	0.81	0.76	92	0.34	0.05	0.80	0.75
−10 to 0 yr	36	0.23	0.05	0.75	0.70	73	0.37	0.09	1.01	0.91	109	0.32	0.05	0.97	0.92
0 to 10 yr	15	0.08	0.00	0.36	0.36	35	0.43	0.00	1.93	1.93	50	0.29	0.00	1.10	1.10
10 to 21 yr	11	0.27	0.00	0.48	0.48	6	0.55	0.13	2.12	1.99	17	0.27	0.10	0.51	0.41
Total	115	0.24	0.04	0.66	0.62	184	0.37	0.07	0.97	0.90	299	0.31	0.05	0.89	0.84

EYO = estimated years to symptom onset; IQR = interquartile range; WMH = white matter hyperintensity.
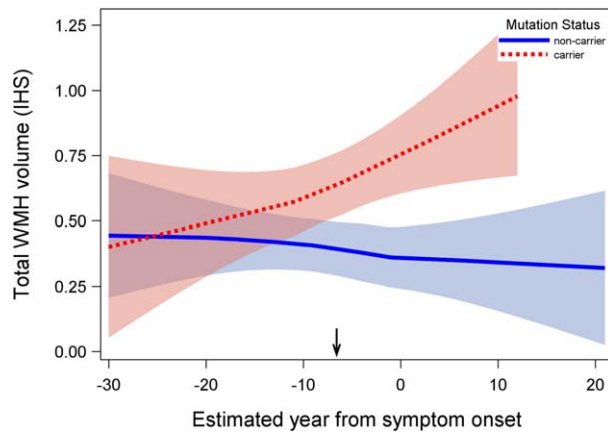
FIGURE 2: Association between estimated year from symptom onset and total WMH volume in mutation carriers and noncarriers. Mutation carriers had greater total WMH volume; differences in WMH volume between groups began increasing systematically approximately 6.6 years before estimated symptom onset (inflection point: –6.6 EYO, indicated by arrow on x-axis). Shaded areas represent 95% confidence intervals. Arrow indicates the inflection point in the analysis. EYO = estimated years to symptom onset; IHS = inverse hyperbolic sine transformation; WMH = white matter hyperintensity. [Color figure can be viewed in the online issue, which is available at www.annalsofneurology.org.]

primary analyses, elevation of WMH associated with mutation status was attenuated. These results first suggest that WMH and $A\beta$ pathology share some degree of dependency. We[24] and others[25,26] have shown previously that WMH volume and markers of fibrillar amyloid pathology are related to each other in the context of LOAD, though others have not.[27] This study confirms that the two biomarkers are related to each other in individuals with definite preclinical AD. Second, they suggest that WMHs do not result primarily from tau-related neurodegeneration, although the extent to which WMHs are related to axonal damage secondary to tau abnormalities cannot be ruled out entirely by these analyses. We showed in ADNI that WMH severity predicts future CSF tau increases and neurodegenerative changes, but that CSF tau levels do not predict future WMH accumulation.[28] We found that CSF $A\beta_{1-42}$ levels appear to be initially higher followed by a rapid decline as a function of EYO in mutation carriers compared to noncarriers (see Fig 3), suggesting that $A\beta_{1-42}$ are abnormally elevated and begin to decline before increases in tau. It is important to note that because the analyses were cross-sectional, the determination of an inflection point was estimated and variable, and we were unable to model the subject-specific trajectories, which would require longitudinal data. Nonetheless, in all cases but 1 (the statistical model in which we controlled for $A\beta_{1-42}$; see Supplementary Table), inclusion of the inflection point significantly

improved the model fit. Furthermore, our approach determined definitively that the relationship between estimated time to symptom onset and WMH volume differed between mutation carriers and noncarriers (i.e., significant mutation status by EYO interactions) and, much like previous work in DIAN,[11] allowed us to compare the evolution of WMH compared with the other biological markers.

WMHs are generally considered markers of small vessel cerebrovascular disease,[29,30] although it is important to point out that nonischemic damage that causes increased fluid motion in discrete areas in the white matter can result in hyperintense signal. Pathogenic mechanisms are not known completely, but a recent genetic meta-analysis suggested a role of blood pressure regulation, $A\beta$-related neurotoxicity, neuroinflammation, and glial cell activation.[31] Pathological correlates, immunohistochemical, and gene expression studies suggest demyelination, axonal loss, gliosis, vacuolation, microglial activation, arteriolosclerosis, and blood brain barrier dysfunction are secondary to ischemic injury in areas appearing radiographically as WMH.[2] The pathophysiology of WMH is likely heterogeneous, and only one study, to our knowledge, has examined the pathological correlates of WMH among individuals with autosomal-dominant forms of AD, in whom the mediators of WMH might differ somewhat.[32] In that report, WMH burden correlated with the severity of cerebral amyloid angiopathy in the temporal lobes, leptomeningeal blood vessel diameter, and lower density of CD68-positive microglia in the parietal lobes among 10 individuals with PSEN1 mutations. Given the propensity for a posterior distribution of WMH we found in mutation carriers, cerebral amyloid angiopathy, which also tends to be distributed in posterior brain regions, is present among individuals with autosomal-dominant forms of AD years before symptoms onset, and correlates with severity of WMH,[33] may be one mediating factor in these observations. Similarly, one previous report suggests that WMH severity correlates with severity of fibrillar forms of amyloid pathology among individuals with CAA, but not LOAD,[34] again suggesting an influence of CAA on the observed relationship between WMH volume and $A\beta_{1-42}$ levels, and we could speculate that CAA may be one causative factor in the parenchymal deposition of $A\beta$. Although in the current study there was some codependency between WMH and presence of at least one cerebral microbleed, the observed increases in WMH among mutation carriers did not appear to be fully mediated by this marker of CAA. Loss of axons, myelin pallor, and diffuse $A\beta$ has also been observed pathologically in white matter of patients with autosomal-dominant AD and LOAD and
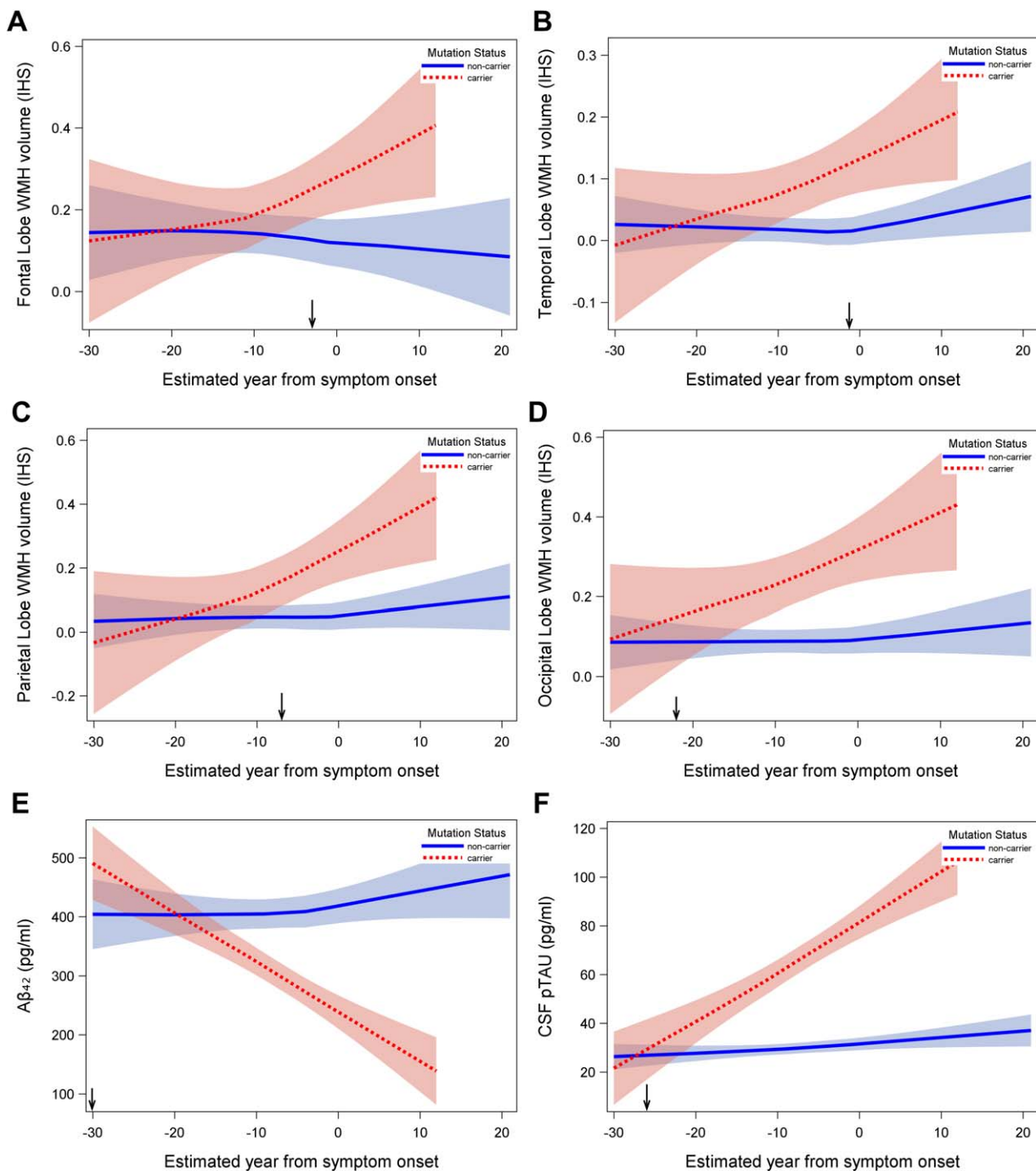
FIGURE 3: Association between estimated year from symptom onset and regional WMH volumes and AD biomarkers in mutation carriers and noncarriers. In all cases, mutation carriers had more-severe biomarker burden; the point at which differences between groups begin to increase systematically (i.e., inflection point) is indicated by an arrow on the x-axis. (A) Frontal lobe WMH volume (inflection point = −3.0 EYO). (B) Temporal lobe WMH volume (inflection point = −1.3 EYO). (C) Parietal lobe WMH volume (inflection point = −7.0 EYO). (D) Occipital lobe WMH volume (inflection point = −22.0 EYO). (E) Aβ$_{42}$ (inflection point = −30.1 EYO). (F) ptau181 (inflection point = −26.0 EYO). Shaded areas represent 95% confidence intervals. Aβ = amyloid beta; AD = Alzheimer's disease; CSF = cerebrospinal fluid; EYO = estimated years to symptom onset; IHS = inverse hyperbolic sine transformation; WMH = white matter hyperintensity. [Color figure can be viewed in the online issue, which is available at www.annalsofneurology.org.]

in animal models of the disease.[35–38] AD-related failure of the axonal machinery attributed to mitochondrial dysfunction, white matter astroglial proliferation, venous collagenosis, and damage to oligodendrocytes and their progenitor cells are other possible pathological correlates of our results.[36,39–42] Clearly, more work relating radiological white matter abnormalities to pathological phenomena is necessary.
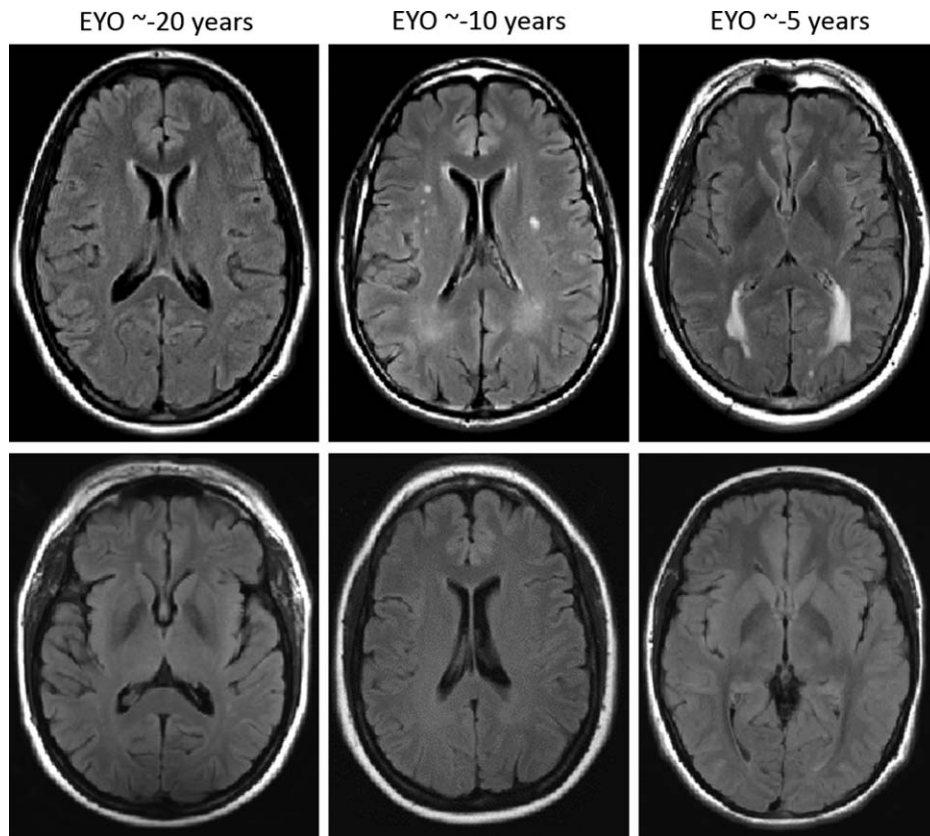
FIGURE 4: Examples of WMH distribution in mutation carriers (upper row) and noncarriers (lower row) across three EYO time points. Top row displays examples of T2-weighted FLAIR MRI scans from 3 mutation carriers at varying estimated years from symptom onset. Bottom row displays examples of MRI scans from noncarriers matched for estimated years from symptom onset (based on parental age of onset). All participants displayed in this figure had CDR scores of 0 at the time of MRI scan. CDR = Clinical Dementia Rating scale; EYO = estimated years to symptom onset; FLAIR = fluid-attenuated inversion recovery; MRI = magnetic resonance imaging; WMH = white matter hyperintensity.

WMHs are quite common in normal aging[43] and have been implicated in non-AD forms of cognitive impairment and dementia.[44] Thus, the question of the extent to which WMHs represent a specific biomarker for AD or for its clinical instantiation is valid and consistent with the conceptualization of other AD biomarkers. For example, increased Aβ pathology is observed in up to 40% of older individuals with no evidence of dementia[45,46]; tau pathology is common in aging, several neurodegenerative diseases, and chronic traumatic brain injury,[47–49] albeit with differing regional patterns across conditions; and regional atrophy is characteristic of LOAD,[50] but is also common in normal aging.[51] Our observations, together with previous work that has implicated WMH in late-onset AD, suggest the possibility that WMH could be incorporated more formally into proposed hypothetical models of disease pathogenesis, such as those proposed by Jack et al.[4] The definitive relationship we observed between increased WMH and autosomal-dominant forms of AD should motivate continued research on the involvement of white matter abnormalities with the disease, including examina-tion of mechanistic interactions with other putative AD biomarkers.

Author Contributions

S.L., F.V., M.E.Z., G.T., T.L.S.B., R.J.B., J.C.M., R.M., and A.M.B. were responsible for conception and design of the study. S.L., A.N., G.T., T.L.S.B., D.S.M., A.M.F., A.G., N.C.F., N.J.C., D.M.H., V.B., B.G., E.M., R.N.M., A.J.S., C.L.M., J.M.R., N.S.R., S.F., C.L., P.R.S., R.A.S., S.S., S.C., C.J., M.W., R.J.B., J.C.M., R.M., and A.M.B. were responsible for acquisition/analysis of data. S.L., F.V., M.E.Z., G.T., and A.M.B. were responsible for drafting manuscript or figures. S.L. and F.V. contributed equally to this work.

Potential Conflicts of Interest

References

1. Debette S, Markus HS. The clinical importance of white matter hyperintensities on brain magnetic resonance imaging: systematic review and meta-analysis. BMJ. 2010;341:c3666.

2. Wardlaw JM, Valdés Hernández MC, Muñoz-Maniega S. What are white matter hyperintensities made of? Relevance to vascular cognitive impairment. J Am Heart Assoc 2015;4:001140.

3. Brickman AM. Contemplating Alzheimer's disease and the contribution of white matter hyperintensities. Curr Neurol Neurosci Rep 2013;13:415.

4. Jack CR, Jr., Knopman DS, Jagust WJ, et al. Tracking pathophysiological processes in Alzheimer's disease: an updated hypothetical model of dynamic biomarkers. Lancet Neurol 2013;12:207–216.

5. Lindemer ER, Salat DH, Smith EE, et al.; Alzheimer's Disease Neuroimaging Initiative. White matter signal abnormality quality differentiates mild cognitive impairment that converts to Alzheimer's disease from nonconverters. Neurobiol Aging 2015;6:2447–2457.

6. Brickman AM, Provenzano FA, Muraskin J, et al. Regional white matter hyperintensity volume, not hippocampal atrophy, predicts incident Alzheimer disease in the community. Arch Neurol 2012;69:1621–1627.

7. Zlokovic BV. Neurovascular pathways to neurodegeneration in Alzheimer's disease and other disorders. Nat Rev Neurosci 2011;12:723–738.

8. White L. Brain lesions at autopsy in older Japanese-American men as related to cognitive impairment and dementia in the final years of life: a summary report from the Honolulu-Asia aging study. J Alzheimers Dis 2009;18:713–725.

9. Schneider JA, Arvanitakis Z, Bang W, Bennett DA. Mixed brain pathologies account for most dementia cases in community-dwelling older persons. Neurology 2007;69:2197–2204.

10. Cairns NJ, Perrin RJ, Franklin EE, et al. Neuropathologic assessment of participants in two multi-center longitudinal observational studies: The Alzheimer Disease Neuroimaging Initiative (ADNI) and the Dominantly Inherited Alzheimer Network (DIAN). Neuropathology 2015;35:390–400.

11. Bateman RJ, Xiong C, Benzinger TL, et al. Clinical and biomarker changes in dominantly inherited Alzheimer's disease. N Engl J Med 2012;367:795–804.

12. Ryman DC, Acosta-Baena N, Aisen PS, et al. Symptom onset in autosomal dominant Alzheimer disease: a systematic review and meta-analysis. Neurology 2014;83:253–260.

13. Morris JC, Aisen PS, Bateman RJ, et al. Developing an international network for Alzheimer research: The Dominantly Inherited Alzheimer Network. Clin Investig (Lond) 2012;2:975–984.

14. Morris JC, Ernesto C, Schafer K, et al. Clinical dementia rating training and reliability in multicenter studies: the Alzheimer's Disease Cooperative Study experience. Neurology 1997;48:1508–1510.

15. Jack CR, Jr., Bernstein MA, Borowski BJ, et al. Update on the magnetic resonance imaging core of the Alzheimer's disease neuroimaging initiative. Alzheimers Dement 2010;6:212–220.

16. Brickman AM, Zahodne LB, Guzman VA, et al. Reconsidering harbingers of dementia: progression of parietal lobe white matter hyperintensities predicts Alzheimer's disease incidence. Neurobiol Aging 2015;36:27–32.

17. Knudsen KA, Rosand J, Karluk D, Greenberg SM. Clinical diagnosis of cerebral amyloid angiopathy: validation of the Boston criteria. Neurology 2001;56:537–539.

18. McZgee VE, Carleton WT. Piecewise regression. J Am Stat Assoc 1970;65:1109–1124.

19. Kim HJ, Yu B, Feuer EJ. Selecting the number of change-points in segmented line regression. Stat Sin 2009;19:597–609.

20. Piepho HP, Ogutu JO. Inference for the break point in segmented regression with application to longitudinal data. Biometr J 2003;45:591–601.

21. Cleveland WS. Robust locally-weighted regression and smoothing scatterplots. J Am Stat Assoc 1979;74:829–836.

22. Burbridge JB, Magee L, Robb AL. Alternative transformations to handle extreme values of the dependent variable. J Am Stat Assoc 1988;83:123–127.

23. Prins ND, Scheltens P. White matter hyperintensities, cognitive impairment and dementia: an update. Nat Rev Neurol 2015;11:157–165.

24. Brickman AM, Guzman VA, Gonzalez-Castellon M, et al. Cerebral autoregulation, beta amyloid, and white matter hyperintensities are interrelated. Neurosci Lett 2015;592:54–58.

25. Grimmer T, Faust M, Auer F, et al. White matter hyperintensities predict amyloid increase in Alzheimer's disease. Neurobiol Aging 2012;33:2766–2773.

26. Zhou Y, Yu F, Duong TQ. White matter lesion load is associated with resting state functional MRI activity and amyloid PET but not FDG in mild cognitive impairment and early Alzheimer's disease patients. J Magn Reson Imaging 2015;41:102–109.

27. Vemuri P, Lesnick TG, Przybelski SA, et al. Vascular and amyloid pathologies are independent predictors of cognitive decline in normal elderly. Brain 2015;138(pt 3):761–771.

28. Tosto G, Zimmerman ME, Hamilton JL, Carmichael OT, Brickman AM; Alzheimer's Disease Neuroimaging Initiative. The effect of white matter hyperintensities on neurodegeneration in mild cognitive impairment. Alzheimers Dement 2015;11:1510–1519.

29. Erten-Lyons D, Woltjer R, Kaye J, et al. Neuropathologic basis of white matter hyperintensity accumulation with advanced age. Neurology 2013;81:977–983.

30. Shim YS, Yang DW, Roe CM, et al. Pathological correlates of white matter hyperintensities on magnetic resonance imaging. Dement Geriatr Cogn Disord 2015;39:92–104.

31. Verhaaren BF, Debette S, Bis JC, et al. Multiethnic genome-wide association study of cerebral white matter hyperintensities on MRI. Circ Cardiovasc Genet 2015;8:398–409.

32. Ryan NS, Biessels GJ, Kim L, et al. Genetic determinants of white matter hyperintensities and amyloid angiopathy in familial Alzheimer's disease. Neurobiol Aging 2015;36:3140–3151.

33. Thanprasertsuk S, Martinez-Ramirez S, Pontes-Neto OM, et al. Posterior white matter disease distribution as a predictor of amyloid angiopathy. Neurology 2014;83:794–800.

34. Gurol ME, Viswanathan A, Gidicsin C, et al. Cerebral amyloid angiopathy burden associated with leukoaraiosis: a positron

emission tomography/magnetic resonance imaging study. Ann Neurol 2013;73:529–536.

35. Takao M, Ghetti B, Murrell JR, et al. Ectopic white matter neurons, a developmental abnormality that may be caused by the PSEN1 S169L mutation in a case of familial AD with myoclonus and seizures. J Neuropathol Exp Neurol 2001;60:1137–1152.

36. Sun SW, Song SK, Harms MP, et al. Detection of age-dependent brain injury in a mouse model of brain amyloidosis associated with Alzheimer's disease using magnetic resonance diffusion tensor imaging. Exp Neurol 2005;191:77–85.

37. Collins-Praino L, Francis Y, Wiegman AF, et al. Soluble amyloid beta levels are elevated in the white matter of Alzheimer's patients, independent of cortical plaque burden. Acta Neuropathol Commun 2014;2:83.

38. Brendza RP, O'Brien C, Simmons K, et al. PDAPP; YFP double transgenic mice: a tool to study amyloid-beta associated changes in axonal, dendritic, and synaptic structures. J Comp Neurol 2003; 456:375–383.

39. Behrendt G, Baer K, Buffo A, et al. Dynamic changes in myelin aberrations and oligodendrocyte generation in chronic amyloidosis in mice and men. Glia 2013;61:273–286.

40. Leuba G, Kraftsik R. Visual cortex in Alzheimer's disease: occurrence of neuronal death and glial proliferation, and correlation with pathological hallmarks. Neurobiol Aging 1994;15:29–43.

41. Reddy PH. Abnormal tau, mitochondrial dysfunction, impaired axonal transport of mitochondria, and synaptic deprivation in Alzheimer's disease. Brain Res 2011;1415:136–148.

42. Pantoni L. Cerebral small vessel disease: from pathogenesis and clinical characteristics to therapeutic challenges. Lancet Neurol 2010;9:689–701.

43. DeCarli C, Massaro J, Harvey D, et al. Measures of brain morphology and infarction in the framingham heart study: establishing what is normal. Neurobiol Aging 2005;26:491–510.

44. Gorelick PB, Scuteri A, Black SE, et al. Vascular contributions to cognitive impairment and dementia: a statement for healthcare professionals from the american heart association/american stroke association. Stroke 2011;42:2672–2713.

45. Bennett DA, Schneider JA, Arvanitakis Z, et al. Neuropathology of older persons without cognitive impairment from two community-based studies. Neurology 2006;66:1837–1844.

46. Aizenstein HJ, Nebes RD, Saxton JA, et al. Frequent amyloid deposition without significant cognitive impairment among the elderly. Arch Neurol 2008;65:1509–1517.

47. DeKosky ST, Blennow K, Ikonomovic MD, Gandy S. Acute and chronic traumatic encephalopathies: pathogenesis and biomarkers. Nat Rev Neurol 2013;9:192–200.

48. Crary JF, Trojanowski JQ, Schneider JA, et al. Primary age-related tauopathy (PART): a common pathology associated with human aging. Acta Neuropathol 2014;128:755–766.

49. McKee AC, Stein TD, Kiernan PT, Alvarez VE. The neuropathology of chronic traumatic encephalopathy. Brain Pathol 2015;25:350–364.

50. Jack CR, Jr., Petersen RC, O'Brien PC, Tangalos EG. MR-based hippocampal volumetry in the diagnosis of Alzheimer's disease. Neurology 1992;42:183–188.

51. Raz N, Lindenberger U, Rodrigue KM, et al. Regional brain changes in aging healthy adults: general trends, individual differences and modifiers. Cereb Cortex 2005;15:1676–1689.